

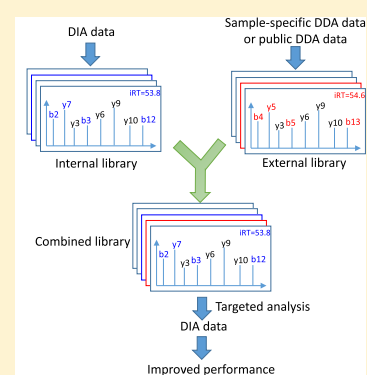
Systematic Assessment of the Effect of Internal Library in Targeted Analysis of SWATH-MS

Chuan-Qi Zhong,^{*,†,§} Rui Wu,[†] Xi Chen,^{‡,§} Suqin Wu,[†] Jianwei Shuai,^{†,||} and Jiahui Han^{*,†}[†]State Key Laboratory of Cellular Stress Biology, Innovation Center for Cellular Signaling Network, School of Life Sciences, Xiamen University, Xiamen 361102, China[‡]Medical Research Institute, Wuhan University, Wuhan 430072, China[§]SpecAly Life Technology Co., Ltd., Wuhan 430072, China^{||}Department of Physics, Xiamen University, Xiamen 361005, China

S Supporting Information

ABSTRACT: Targeted analysis of sequential window acquisition of all theoretical mass spectra (SWATH-MS) requires the spectral library, which can be generated by shotgun mass spectrometry (MS) or by the pseudo-spectra files directly obtained from SWATH-MS data. The external library generated by shotgun MS is employed in most SWATH-MS research. However, performance of the internal library, which is constructed by pseudo-spectra files, in the targeted analysis of SWATH-MS has not been systemically evaluated. Here, we show that up to 40% of the peptides detected by the internal library were not overlapped with those detected by the external library for most SWATH-MS data sets. However, the internal library did not identify extra phosphopeptides compared with the external library for phosphoproteomic SWATH-MS data. Therefore, the internal library should be incorporated into the external library for targeted analysis of non-phosphoproteomic SWATH-MS, given that it can significantly increase the number of peptides of SWATH-MS without requiring additional instrument measurement time.

KEYWORDS: SWATH-MS, data-independent acquisition, spectral library, OpenSWATH, DIA-Umpire, Group-DIA, tumor necrosis factor, L929 cells, plasma, phosphoproteomics



INTRODUCTION

In recent years, mass spectrometry (MS)-based proteomics has shifted from identification of proteins in one sample to quantification of proteins across multiple samples.¹ Identification of proteins is typically accomplished by shotgun MS (also referred to as data-dependent acquisition, DDA), where tryptic peptides were selected for fragmentation depending on the peptide MS1 intensity. This undersampling nature of DDA results in frequent missing values, especially for low-signal peptides. This drawback of shotgun MS has impaired application of the MS technique to life science research as many studies are focusing on quantitative differences between biological conditions rather than cataloging protein contents. To alleviate this missing value problem, several alternative MS workflows have been proposed, such as targeted MS methods (selected or parallel reaction monitoring^{2–4}) and data-independent acquisition (DIA).^{5–8}

In DIA mass spectrometry, the peptide ion range is divided into several predetermined subranges, each of which is fragmented and scanned as a whole.⁹ In this scanning mode, the link between the precursor ion and product ions is missing, which is challenging for traditional MS search strategies. Recently, the interception of DIA-MS data is facilitated by the use of a targeted approach, whereby a preexisting peptide assay library is used to identify specific peptides.¹⁰ Peptide libraries are

typically generated through the collection of shotgun MS results, which are converted into a spectral library where all peptide ions are represented by a reference spectrum. Therefore, the targeted analysis of DIA-MS data is critically dependent on the composition and depth of the assay library. To build a deeper peptide library, a common way is to increase the depth of proteome coverage in DDA by intensive fractionation of peptides. Several studies have demonstrated that targeted analysis with the extensive spectral library can identify more peptides than that with the single DDA run library.^{11–14} Furthermore, the global or species-specific libraries (SSLs) generated by large-scale DDA runs are available for targeted analysis of sequential window acquisition of all theoretical mass spectra (SWATH-MS).^{15–18} More recently, a synthetic proteotypic peptide assay library representing the complete human proteome has been published.¹⁹

Alternatively, the peptide library can also be constructed directly from DIA-MS files, and that strategy is also referred to as the “library-free” strategy.^{20–23} DIA-Umpire and Group-DIA are software tools designed for deconvolution of chimeric tandem mass spectra in DIA-MS data into pseudo-DDA MS spectra.^{20,21} Specifically, extracted-ion chromatograms (XICs)

Received: October 5, 2019

Published: October 30, 2019

of MS1 and MS2 ions are first compared. Subsequently, one MS1 ion, together with the product ions whose XICs show high similarity with that of the MS1 ion, is constructed into a DDA-like spectrum. These pseudo-spectra files are searched and built as a spectral library, which is usually named the internal library. Internal libraries provide several inherent advantages over the libraries built from DDA runs: (1) retention times (RTs) of peptides in internal libraries are the same as those in DIA-MS data; (2) fragmentation patterns of product ions in internal libraries are closer to those in DIA-MS data compared with the DDA libraries. In addition, internal libraries provide many extra peptides that cannot be detected by DDA libraries.²⁴ However, several studies showed that internal-library-based targeted analysis usually identified less peptides compared with a DDA-library-based strategy.^{12,24}

In an effort to assess the influence of the internal library on targeted SWATH-MS analysis, we acquired six SWATH-MS data sets, namely, mouse cell line lysate samples, human cell line lysate samples, immunoprecipitation samples, human plasma samples, and phosphoproteomic samples. Two SWATH data sets are from the mouse cell line lysate samples, so six SWATH data sets are from five sample types. In all data sets, DDA libraries yielded more peptide identification compared with internal libraries. More importantly, the combined libraries, merged with DDA libraries and internal libraries, can provide 15–58 and 10–15% improvement in peptide and protein identification, respectively, compared with DDA libraries alone. In a typical targeted analysis workflow of SWATH-MS, the external library is generated. We propose that internal libraries should be merged with the external library, and the combined library can significantly increase the peptide number without the need for extra sample and instrument running time.

METHODS

Sample Preparation for MS Analysis

- (1) L929 100 variable window (VW) samples: Murine L929 cells were seeded at 0.5×10^6 cells per well on the 12-well plate in Dulbecco's modified Eagle's medium (DMEM) supplemented with 10% fetal bovine serum (FBS). After 12 h, L929 cells were treated with tumor necrosis factor (TNF) at 10 ng/mL for different time points. Cells were washed with phosphate-buffered saline (PBS) three times, and 100 μ L of lysis buffer [1% sodium deoxycholate (SDC), 10 mM tris(2-carboxyethyl)phosphine (TCEP), 40 mM chloroacetamide (CAA), 100 mM Tris-HCl, pH 8.5] was added into one well. The lysed cells were collected into the 1.5 mL Eppendorf (EP) tube, which was subjected to 95 °C heat for 5 min and then sonicated. Subsequently, 1% SDC was diluted into 0.5% with water. The protein concentration was measured with the Pierce 660 nm protein assay reagent (Thermo). Trypsin (Sigma) was added at the ratio of 1:100 (trypsin/protein). The tubes were kept at 37 °C for 12–16 h. Peptides were desalted with styrene divinylbenzene-reverse phase sulfonate (SDB-RPS) StageTips.
- (2) HeLa samples: HeLa cells were seeded at 1×10^5 cells per well on the 24-well plate in DMEM supplemented with 10% FBS. After 12 h, HeLa cells were treated with TNF at 10 ng/mL for different time points. Cells were lysed, collected, and digested as described above.
- (3) Tumor necrosis factor receptor 1 (TNFR1) immunoprecipitation samples: L929 cells were seeded at 1×10^7 cells

per 15 cm dish in DMEM supplemented with 10% FBS. After 24 h, the cells were treated with 10 μ g/mL 3 \times Flag-TNF for different time points. Cells were stimulated with 3 \times Flag-TNF for 0, 5, 15, 30, 45, and 60 min. For each time-point experiment, cells in ten 15 cm dishes were collected. After TNF treatment, cells were immediately washed twice with PBS and harvested by scraping and centrifugation at 100 g for 10 min. The harvested cells were washed with PBS and lysed for 30 min on ice in HBS lysis buffer (12.5 mM *N*-(2-hydroxyethyl)piperazine-*N'*-ethanesulfonic acid, 150 mM NaCl, 1% Nonidet P-40, pH 7.5) with a protease inhibitor cocktail. Cell lysates were then spun down at 20 000g for 30 min. The soluble fraction was collected and immunoprecipitated overnight with anti-Flag M2 antibody-conjugated agarose at 4 °C. Resins containing protein complexes were washed three times with HBS lysis buffer. Proteins were then eluted twice with 0.15 mg/mL of 3 \times Flag peptide in HBS lysis buffer for 15 min each time, and elutions were pooled for a final volume of 300 μ L. Proteins in the elution were precipitated with 20% trichloroacetic acid, and the pellet was washed twice with 1 mL of cold acetone and dried in SpeedVac. The protein pellet was dissolved in 1% SDC/10 mM TCEP/40 mM CAA/Tris-HCl pH 8.5. Digestion was performed as described above.

- (4) Phosphoproteomic samples: L929 cells were seeded at 1×10^6 at one well in a six-well plate in DMEM supplemented with 10% FBS. After 24 h, cells were treated with 10 ng/mL TNF for 0, 0.5, 1, 2, 3, and 4 h. Cells were collected in biological duplicates. After TNF treatment, cells were washed with ice-cold PBS three times. A 200 μ L lysis buffer was added into one well. The lysed cells were transferred to 1.5 mL EP tubes, which were subjected to 95 °C heat for 5 min and sonicated. The protein concentration was measured with a Pierce 660 nm protein assay reagent (Thermo). Then, 200 μ g of proteins was used for digestion. Trypsin (Sigma) was added at the ratio of 1:100 (trypsin/protein). The tubes were kept at 37 °C for 12–16 h. After digestion, phosphopeptides were enriched using TiO₂. Briefly, peptide solutions were added with an equal volume of 4% trifluoroacetic acid (TFA)/2 mM KH₂PO₄/isopropanol (ISO).²⁵ After removing the pellet by centrifugation of 12 000 rpm for 5 min, the supernatants were used for enrichment. Next, 5 mg of TiO₂ was added into one digestion solution. The tubes were incubated at 40 °C and shaken (2000 rpm) for 5 min. Beads were collected by centrifugation, and the supernatant was discarded. The beads were washed with 500 μ L of 2% TFA/50% ISO three times. Phosphopeptides were then eluted with 60 μ L of 20% NH₃·H₂O/32% acetonitrile (ACN), followed by concentration using an evaporative concentrator. Phosphopeptides were then desalted using SDB-RPS StageTips.
- (5) Human plasma samples: Blood was taken by lancets (Vitrex Sterilance Lite II) to obtain small quantities of capillary blood, and 5 μ L of blood was transferred to a PCR tube containing 0.56 μ L of 106 mM trisodium citrate. The blood was centrifuged for 15 min at 2000g, and plasma was harvested. The protein concentration in human plasma was measured with the Pierce 660 nm protein assay reagent (Thermo). For high-pH reverse-phase fractionation, about 400 μ g of proteins was digested. Two immunodepletion kits (Thermo 85164

and Bio-RAD 7326708) were used for removal of the high abundance plasma proteins with the purpose of building a deep human plasma spectral library. Mouse plasma was added into 100 μ L of lysis buffer [1% sodium deoxycholate (SDC), 10 mM tris(2-carboxyethyl)-phosphine (TCEP), 40 mM chloroacetamide, 100 mM Tris-HCl, pH 8.5]. The tubes were subjected to 95 °C heat for 5 min. Subsequently, 1% SDC was diluted into 0.5% with water. Trypsin (Sigma) was added at the ratio of 1:100 (trypsin/protein). The tubes were kept at 37 °C for 12–16 h. After desalting, about 5 μ g of peptide was loaded for a single SWATH-MS run.

- (6) Mouse plasma samples: Protein concentrations of mouse plasma samples were measured with a Pierce 660 nm protein assay reagent (Thermo). First, 1 μ L of mouse plasma was added into 100 μ L of lysis buffer (1% sodium deoxycholate (SDC), 10 mM tris(2-carboxyethyl)-phosphine (TCEP), 40 mM chloroacetamide, 100 mM Tris-HCl, pH 8.5). The tubes were subjected to 95 °C heat for 5 min. Subsequently, 1% SDC was diluted into 0.5% with water. Trypsin (Sigma) was added at the ratio of 1:100 (trypsin/protein). The tubes were kept at 37 °C for 12–16 h. Peptides were desalted with SDB-RPS StageTips.

■ EXPERIMENTAL DESIGN AND STATISTICAL RATIONALE

L929 25 Da data set: 8 treatment conditions, 3 biological replicates per condition, 24 samples in total.

L929 100 VW data set: 10 treatment conditions, 12 samples in total.

HeLa data set: 7 treatment conditions, 3 biological replicates per condition, 21 samples in total.

Human plasma data set: 2 biological samples, 3 technical injections.

Mouse plasma data set: 4 treatment conditions, 2–3 biological replicates per condition, 10 samples in total.

Phosphopeptidomics data set: 6 treatment conditions, 2 biological replicates per condition, 12 samples in total.

All protein or phosphopeptide intensities were input into Perseus software. The statistical analysis was performed using the default settings.

SWATH-MS Analysis

Peptides were dissolved in 0.1% formic acid (FA) and analyzed with SWATH-MS. MS analysis was performed on TripleTOF 5600 (Sciex) mass spectrometry coupled to a NanoLC Ultra 2D Plus (Eksigent) high-performance liquid chromatography system. Peptides were first bound to a 5 mm \times 500 μ m trap column packed with Zorbax C18 5 μ m 200 Å resin using 0.1% (v/v) formic acid/2% acetonitrile in H₂O at 10 μ L/min for 5 min and then separated using a gradient from 2 to 35% buffer B [buffer A: 0.1% (v/v) formic acid, 5% dimethyl sulfoxide (DMSO) in H₂O; buffer B: 0.1% (v/v) formic acid, 5% DMSO in acetonitrile] on a 35 cm \times 75 μ m in-house pulled emitter-integrated column packed with Magic C18 AQ 3 μ m 200 Å resin. The gradient time is 180 min for L929, HeLa, and plasma data sets, 240 min for the IP data set, and 60 min for the phosphoproteomic data set. For SWATH-MS, the mass spectrometer was operated such that a 250 ms survey scan [time-of-flight mass spectrometry (TOF-MS)], which was collected in 350–1500 m/z , was performed followed by 32 100 ms MS2 experiments or 100 33 ms MS2 experiments. MS2

scans were collected in 100–1800 m/z . The fixed 25 Da MS2 experiments used an isolation width of 26 m/z (containing 1 m/z for the window overlap) to cover the precursor mass range of 400–1200 m/z .

The 100 variable isolation windows are “399.5–409.9, 408.9–418.9, 417.9–427.4, 426.4–436, 435–443.6, 442.6–450.8, 449.8–458, 457–464.8, 463.8–471.1, 470.1–476.9, 475.9–482.8, 481.8–488.6, 487.6–494, 493–499, 498–504.4, 503.4–509.3, 508.3–514.3, 513.3–519.2, 518.2–524.2, 523.2–529.1, 528.1–534.1, 533.1–539, 538–543.5, 542.5–548.5, 547.5–553, 552–558, 557–562.5, 561.5–567, 566–571.5, 570.5–576, 575–580.5, 579.5–585, 584–589.5, 588.5–594, 593–598, 597–602.5, 601.5–607, 606–611.1, 610.1–615.6, 614.6–620.1, 619.1–624.6, 623.6–628.6, 627.6–633.1, 632.1–637.6, 636.6–642.1, 641.1–646.6, 645.6–651.1, 650.1–655.6, 654.6–660.1, 659.1–665.1, 664.1–669.6, 668.6–674.5, 673.5–679, 678–684, 683–688.5, 687.5–693.4, 692.4–698.4, 697.4–703.3, 702.3–708.7, 707.7–713.7, 712.7–719.1, 718.1–724.5, 723.5–729.9, 728.9–735.3, 734.3–740.7, 739.7–746.5, 745.5–751.9, 750.9–757.8, 756.8–763.6, 762.6–769.5, 768.5–775.3, 774.3–781.2, 780.2–787, 786–793.3, 792.3–800.1, 799.1–806.4, 805.4–813.1, 812.1–820.3, 819.3–827.5, 826.5–835.2, 834.2–843.3, 842.3–851.4, 850.4–859.9, 858.9–868.9, 867.9–878.4, 877.4–888.3, 887.3–899.1, 898.1–910.3, 909.3–922.9, 921.9–936, 935–949.5, 948.5–963.4, 962.4–978.7, 977.7–994.9, 993.9–1015.6, 1014.6–1042.2, 1041.2–1070.1, 1069.1–1100.7, 1099.7–1140.7, 1139.7–1196.5.”

Shotgun MS Analysis and the Spectral Library Building

Data-dependent acquisition was performed on two instruments. DDA for generation of the L929 library and SSL in the TNFR1 IP data set were performed on TripleTOF 5600 (Sciex). DDA for generation of SSL in the HeLa data set was performed on TripleTOF 5600 (Sciex) and timsTOF Pro (Bruker Daltonics). Liquid chromatography used in DDA on 5600 was the same as that in SWATH-MS described above. For timsTOF pro, an ultrahigh-pressure nanoflow chromatography system (Elite UHPLC, Boker) was coupled. Liquid chromatography was performed on a reversed-phase column (40 cm \times 75 μ m i.d.) at 50 °C packed with Magic C18 AQ 3 μ m 200 Å resin with a pulled emitter tip. Solution A is 0.1% FA in H₂O, and solution B is 0.1% FA in ACN. In 120 min experiments, peptides were separated with a linear gradient from 0 to 5% B within 5 min, followed by an increase to 30% B within 105 min and further to 35% B within 5 min, followed by a washing step at 95% B and re-equilibration. timsTOF pro was operated in the PASEF mode.^{26,27} The Bruker. tdf raw files were converted to mgf files with vendor convert software.

Wiff files from 5600 were converted to mgf files using the qtofpeakpicker tool in proteoWizard MSConvert software (v.3.0.447).²⁸ The mgf files from 5600 and those from timsTOF pro were converted to mzML files using proteoWizard MSConvert software. The mzML files were analyzed using Trans-Proteomic Pipeline (TPP, version 5.0) software.²⁹ mzML files were subjected to database search using Comet (version 2017.01)³⁰ and X!tandem (version 2013.06.15.1, native and *k*-score)³¹ against Swiss-Prot human (downloaded in September 2018) appendant with common contaminants and reversed sequence decoys (41 298 entries including decoys for human). The search parameters were set as follows: parent monoisotopic tolerance 50 ppm, product ion tolerance 0.1 Da for 5600 and 0.05 Da for timsTOF, modification Carbamidomethyl on cysteine (57.021464@C), potential modification oxidation on

methionine (15.994915@M), and maximum missed cleavage sites 2. The pep.xml search results were validated and scored using PeptideProphet³² with parameters -OARPd -dDECOY and combined by iProphet³³ with parameters DECOY = DECOY. Mayu (version 1.07)³⁴ was used to determine iProphet probability corresponding to 1% protein false discovery rate (FDR). For the deep human plasma library, the peptides filtered at 1% protein FDR were input into ProteinProphet³⁵ for generating a protein list. The peptide ions passing the 1% FDR were input into SpectraST³⁶ for library building with collision-induced dissociation (CID)-quadrupole TOF (QTOF) setting. For phosphoproteomics data, iProphet results were analyzed with PTMProphet for phosphorylation site localization. The phosphopeptides with PTMprophet score >0.7 were kept for spectral library building. The retention time of peptides in the sptxt file was replaced with the iRT time using spectrast2spectrast_irt.py script (downloaded from www.openswath.org), and the peptides used for retention time normalization were endogenous peptides or spiked-in iRT peptides. The sptxt file was made a consensus nonabundant spectral library with the iRT retention time using spectraST.

Internal Libraries Generated by Group-DIA and DIA-Umpire Software

SWATH-MS wiff files were converted to centroid mzXML using the qtofpeakpicker tool and profile mzXML files using proteoWizard MSConvert v.3.0.447. Centroid mzXML files were analyzed with DIA-Umpire.²⁰ DIA-Umpire was run with default setting except for BoostComplementaryIon = false. Profile mzXML files were split into a number of MS2 mzXML files and the 1 MS1 mzXML file according to the SWATH window using the in-house script. For the L929 25 Da data set, 24 180 min gradient runs were collectively analyzed. For the L929 100 VW data set, 12 180 min gradient runs were analyzed together. For the HeLa data set, 21 180 min gradient runs were analyzed together. For the IP data set, 12 240 min gradient runs were analyzed together. For the plasma data set, 6 180 min gradient runs or 10 180 min gradient runs were analyzed together. Group-DIA software was composed of four modules: alignment, analysis, identification, and validation. For generation of the internal library, only “alignment” and “analysis” modules were performed. Retention time in multiple runs was first aligned using MS1 intensity. MS1 and MS2 features were first extracted in a single run and then concatenated across all runs. Precursors’ and product ions’ XICs similarities were compared, and the pairs of precursors and product ions were then extracted. The generated pseudo-spectra were stored in mgf and mzML formats.

The mgf files from DIA-Umpire and Group-DIA were converted to mzML files, which were analyzed with Trans-Proteomic Pipeline (TPP, version 5.0) software. mzML files were subjected to database search using Comet (version 2017.01) and X!tandem (version 2013.06.15.1, native and *k*-score) against Swissprot mouse or human (both downloaded in September 2018) appendant with common contaminants and reversed sequence decoys (34 492 entries including decoys for mouse; 41 298 entries including decoys for human). The search parameters were set as follows: parent monoisotopic tolerance 50 ppm, product ion tolerance 0.1 Da, carbamidomethyl on cysteine (57.021464@C), potential modification oxidation on methionine (15.994915@M), and maximum missed cleavage sites 2. The pep.xml search results were validated and scored using PeptideProphet with parameters -OARPd -dDECOY and

combined by iProphet with parameters DECOY = DECOY. Mayu (version 1.07) was used to determine iProphet probability corresponding to 1% peptide FDR. The peptide ions passing the 1% FDR were input into SpectraST for library building with CID-QTOF setting. The retention time of peptides in the sptxt file was replaced with the iRT time using the spectrast2spectrast_irt.py script (downloaded from www.openswath.org), and iRT peptides used for retention time normalization were endogenous peptides. The sptxt file was made a consensus nonabundant spectral library with the iRT retention time using spectraST.

Merging of Internal Library and DDA Libraries

We found that the combined library generated with SpectraST,³⁶ regardless of the option employed in SpectraST such as -cJU, -cJI, -cJS, -cJH, and -cJA, can miss a fraction of peptides that has been detected by the separate library (Figure S15A). This result was apparently not reasonable. Thus, we wrote an in-house script to merge different libraries. Briefly, the peptides that have been identified by OpenSWATH at 1% global protein FDR were extracted from the separate library, followed by combination. When the repeat peptides were encountered, the peptides in the internal library were taken in priority. The combined library was subsequently subjected to OpenSWATH-PyProphet-TRIC workflow analysis.

To examine whether the precursor ions in the combined library passed the threshold of 1% protein FDR, we re-searched all raw files including 286 DDA files and 24 pseudo-DDA files (for fixed windows SWATH-MS data set), resulting in 8531 proteins at 1% protein FDR as determined by Mayu. The precursors in the combined library were compared with those in the 8531 proteins. In the re-search library, 97.6% (19 011 of 19 486) of the total peptides in the combined library were included, while 98.5% (2973 of 3013) of the proteins composed of proteotypic peptides in the combined library were found in the re-search library (Figure S15B). Although we cannot conclude that 1% protein FDR was achieved for the combined library, these results showed that the vast majority of precursors in the combined library have high confidence.

Targeted Analysis of SWATH-MS Using OpenSWATH-PyProphet-TRIC Workflow

The consensus sptxt files were converted to tsv using spectrast2tsv.py script, which was then converted to a TraML file with a TargetedFileConverter tool, which is integrated into OpenMS software (version 2.2.0).³⁷ In OpenSWATH analysis, ciRT peptide³⁸ and iRT peptides³⁹ were used for retention time normalization. The XIC extraction window is 20 min. An extended version of PyProphet^{40,41} (PyProphet-cli v0.19, <https://github.com/PyProphet>) was employed for FDR estimation. Then, 1% protein FDR at the global level was applied in the nonphosphoproteomic data set, and 1% global peptide FDR was set for the phosphoproteomic data set. The filtered results were input into TRIC software for cross-run alignment. The parameters in TRIC⁴² were set as follows: --method LocalMST --realign_method lowess_cython --max_rt_diff 60 --mst:useRTCorrection True --mst:Stdev_multiplier 3.0 --target_fdr 0.01 --max_fdr_quality 0.05.

It has been reported⁴³ that the comprehensive spectral library contains many peptides (named false-negative peptides) that do not exist in the DIA data, for which the multiple testing in the data analysis needs to be corrected. This issue leads to the loss of many true signals, thereby reducing the confidence of the original peptide assignment. The issue of false-negative peptides

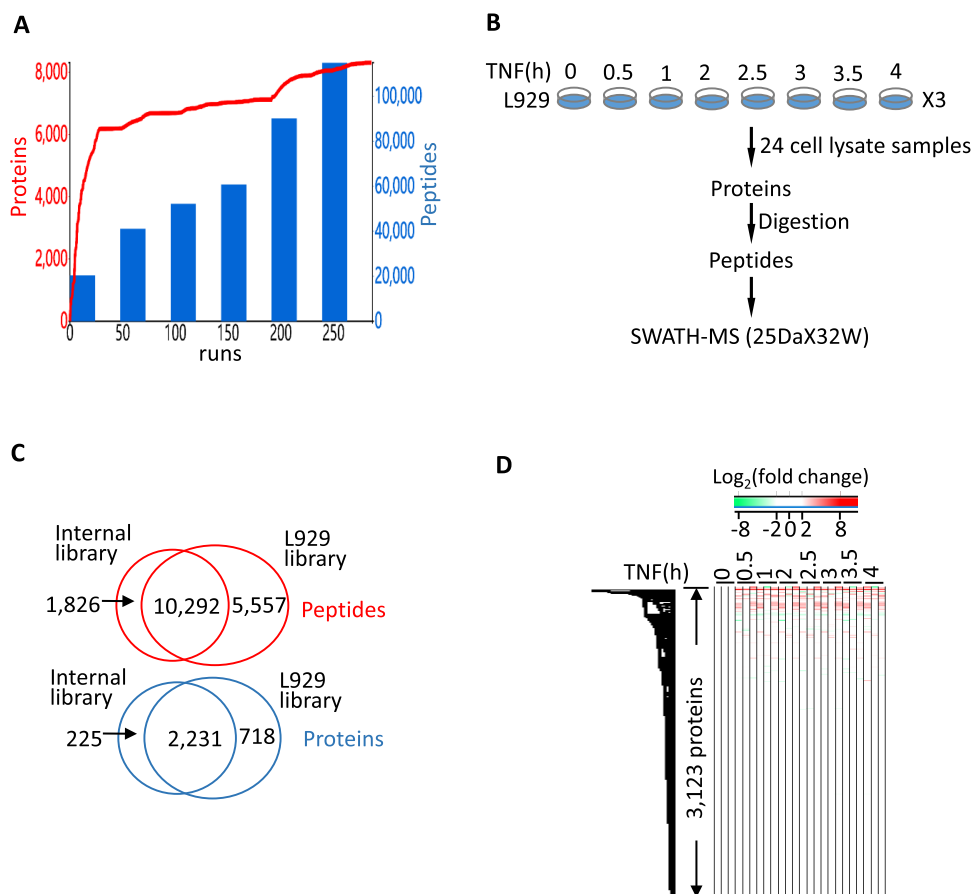


Figure 1. Peptides detected by the extensive external library covered those by the internal library for fixed-window SWATH-MS data. (A) Cumulative identification of protein and peptide numbers across 286 DDA runs during building of the L929 library. (B) Experimental scheme of L929 cells under TNF treatment for various time points. (C) Overlap of quantified peptides or proteins by the internal library and the L929 library at 1% global protein FDR. (D) Heatmap of quantified protein intensities by the combined library across 24 samples.

can be partially alleviated by applying a subset of the comprehensive library, which only contained the proteins detected in the samples. This strategy is similar to our approach, by which we extracted the proteins from the library filtered by 1% global protein FDR. Although there are two steps of targeted DIA data analysis in our approach, the final results have been rigorously filtered.

Protein Inference and Quantification

The TRIC results were used for protein inference and quantification. First, proteins with proteotypic peptides were considered as “uniquely identified”, and the proteotypic peptides accounted for about 90% of all identified peptides (Table S1). Second, the peptides mapped to more than one protein entry were handled as follows:

1. The peptides shared with the proteins with proteotypic peptides were excluded for protein inference and quantification.
2. The peptides without evidence of unique protein mapping were considered as “from one protein representing the gene locus and expressed as the alphabetically first entry of the protein database (gene locus identification).”

To generate a complete quantitative matrix of the IP data set, peptides identified in all biological replicates of at least one time point were kept for extraction of quantitative information.

Peptide intensities were directly from TRIC output results, where peptide intensities were calculated by summing the top five most intense fragment ion peak areas. In each data set, all identified peptides from the specific protein are ranked by the average intensity in all runs. Subsequently, the top three intense peptides of the specific protein are selected, and the sum of these three peptide intensities represents the protein intensity in each run. Where <3 peptides were detected, the available peak groups were summed.

We found that a large number of missing values of protein quantitation was detected when the comprehensive library was used. This was caused neither by stochastic precursor ion selection as in shotgun MS because SWATH-MS recorded all precursor ions, nor by false-positive identification as 1% protein FDR at the global level was applied. The intensity of a specific peptide that is not detected by OpenSWATH was calculated as zero, and “zero” values were obviously inconvenient for downstream bioinformatics processing. Instead of missing value imputation, we used “background intensity strategy” to address this issue. The background intensity strategy was performed as follows:

1. If one peptide was detected in run A but not in run B, the retention time (RT) of the peptide in run A was used for location of the peptide in run B. The peptide RT in run A was transformed into an iRT value, which was also considered as an iRT value in run B. iRT in run B was then transformed into the actual RT in run B. Considering that

this RT may not be precise, the RT window of the peptide in run B was taken. The RT window of the peptide in B run was calculated by extending 10 min at the center of the RT value.

- In the RT window of the peptide in run B, the product ion *mz* intensities were extracted and summed at each cycle since no peaks were detected across the window. The summed *mz* intensity values were ranked, and the median value was taken. Because there is no peak in the retention time range, the summed intensity of the baseline was significantly lower than other peptide peak intensities. Thus, we compare intensities of 100 peaks to the summed intensities of their baseline in a 20 min retention time window. We found the ratios of “peak intensity” to “the summed intensity of baseline” about 5.5–6.0, and we take the average number “5.7”. The median value was multiplied with 5.7 and considered as background intensity.

Raw MS Data and Spectral Library Availability

The raw MS data and spectral libraries have been deposited into the PeptideAtlas with identifier PASS01314 and can be accessed at <http://www.peptideatlas.org/PASS/PASS01314>.

Animal Plasma and Human Plasma Samples

All animal experimental protocols were approved by the Institutional Animal Care and Use Committee at Xiamen University. Human plasma samples were obtained with approval of the research ethics boards of Xiamen University and Xiamen First Hospital.

RESULTS

Internal Library Supplements Peptides Detected by the Extensive Spectral Library for Fixed-Window SWATH-MS Data

In our previous study, we attempted to identify all expressed proteins in the murine cell line L929.²¹ Through extensive fractionation techniques at protein and peptide levels coupled with shotgun MS (Figure S1), we generated a spectral library (referred to as the L929 library hereafter) with 286 DDA runs, which contained 109 323 striped peptides corresponding to 8599 mouse proteins. As shown in Figure 1A, the number of identified proteins dramatically increased within 50 runs, and then the increase slowed down from 50 runs to 200 runs. When DDA runs were over 200, the number of proteins identified came to saturation, suggesting that it reached the maximum number of proteins identified in the DDA data set in the murine L929 cell line.

We used OpenSWATH⁴⁴ to analyze the SWATH-MS data from L929 cell lysates. Wild-type L929 cells were treated with TNF for different time periods in biological triplicates (Figure 1B). The SWATH-MS data were acquired in the fixed-window (32W × 25 Da) mode. We also analyzed one biological replicate (8 of 24 samples) using shotgun MS, which has been included in the L929 library. Collectively, 2949 proteins were quantified across 24 samples at 1% global protein FDR (Table S1 and Figure S2A). To compare the performance of targeted analysis using the L929 library or the internal library, we applied Group-DIA and DIA-Umpire to generate the pseudo-spectra files directly from SWATH-MS files. The pseudo-spectra files were subjected to database searches, and an internal library was made. Targeted analysis with OpenSWATH using the internal library revealed that 2456 proteins were quantified across 24 samples

(Table S1 and Figure S2B). The coefficients of variations (CVs) of protein intensities in biological replicates were computed. CVs identified by the internal library (Figure S2D) were marginally lower than those by the L929 library (Figure S2C). Pearson's correlation coefficients between two samples using the internal library were slightly higher than those in the L929 library (Figure S3A), suggesting that protein quantification based on the internal library has better reproducibility. We noticed that the correlation between protein intensities using the internal library and those with the external library is relatively poor. Since the protein intensities were calculated by summing the peptide intensities, we extracted the intensities of common peptide precursors identified by both libraries (Figure 1C). Similar to the correlation of proteins from two libraries, the peptide intensities also show a relatively poor correlation (Figure S3B). This indicates that the poor correlation between protein intensities by two libraries might perhaps stem from the discrepant factors of the assay libraries such as retention time or product ions for the same peptide precursor. The top six intense fragment ions of the peptides in spectral libraries will be selected to assemble the assay libraries. The peptide precursors in L929, internal assay libraries as well as identified by both libraries are shown in Figure S4A. We focused on the 10 747 precursors that are identified by two libraries. First, we compared the iRT values of these peptides. iRTs from two libraries were highly reproducible (Figure S4B), suggesting that the retention time is not the cause of the poor correlation of protein intensities. Second, we examined the product ions of the peptides from two libraries. The percentages of the peptide with indicated overlapped product ions from two libraries are shown in Figure S4C. Unexpectedly, the percent of peptides with the same six product ions between two libraries is only about 5%. About 62% of the peptides have three or four overlapped product ions between two libraries. Twenty-eight percent of peptides have five shared product ions. This result suggested that the majority of product ions of peptides that were selected for quantification from two libraries were different. To further demonstrate that the poor correlation of protein intensities results from the different product ions from two libraries, we manually checked the XICs of product ions for several common peptides in two libraries. As shown in Figure S5, different product ions from two libraries showed largely varying intensities. This result confirmed that poor correlation of protein intensities is caused by varying product ions from two libraries.

Subsequently, the quantified peptides and proteins were compared, showing that the L929 library approach can cover 85% (10 292 of 12 118) of the peptides and 91% (2231 of 2456) of the proteins from the internal library strategy (Figure 1C). This result demonstrated that the L929 library was pretty complete for these SWATH-MS data. However, when we used the combination of the L929 library and the internal library, 3123 proteins were quantified (Figure 1D), which is about 7.6% (225 of 2949) and 12% (1826 of 15 849) improvement in the number of quantified proteins and peptides, respectively. The CVs from the combined library are similar to those from the internal library (Figure S6A), which are both lower than those from the L929 library. We compared the proteins and peptide precursors identified by the combined library with those by individual libraries. The combined library covers 99.9% of the proteins detected by the L929 library and 93.1% of the proteins by the internal library (Figure S6B). Moreover, the combined library contains 100% of overlapped proteins of the individual libraries. At the peptide level, the combined library offers 93.6%

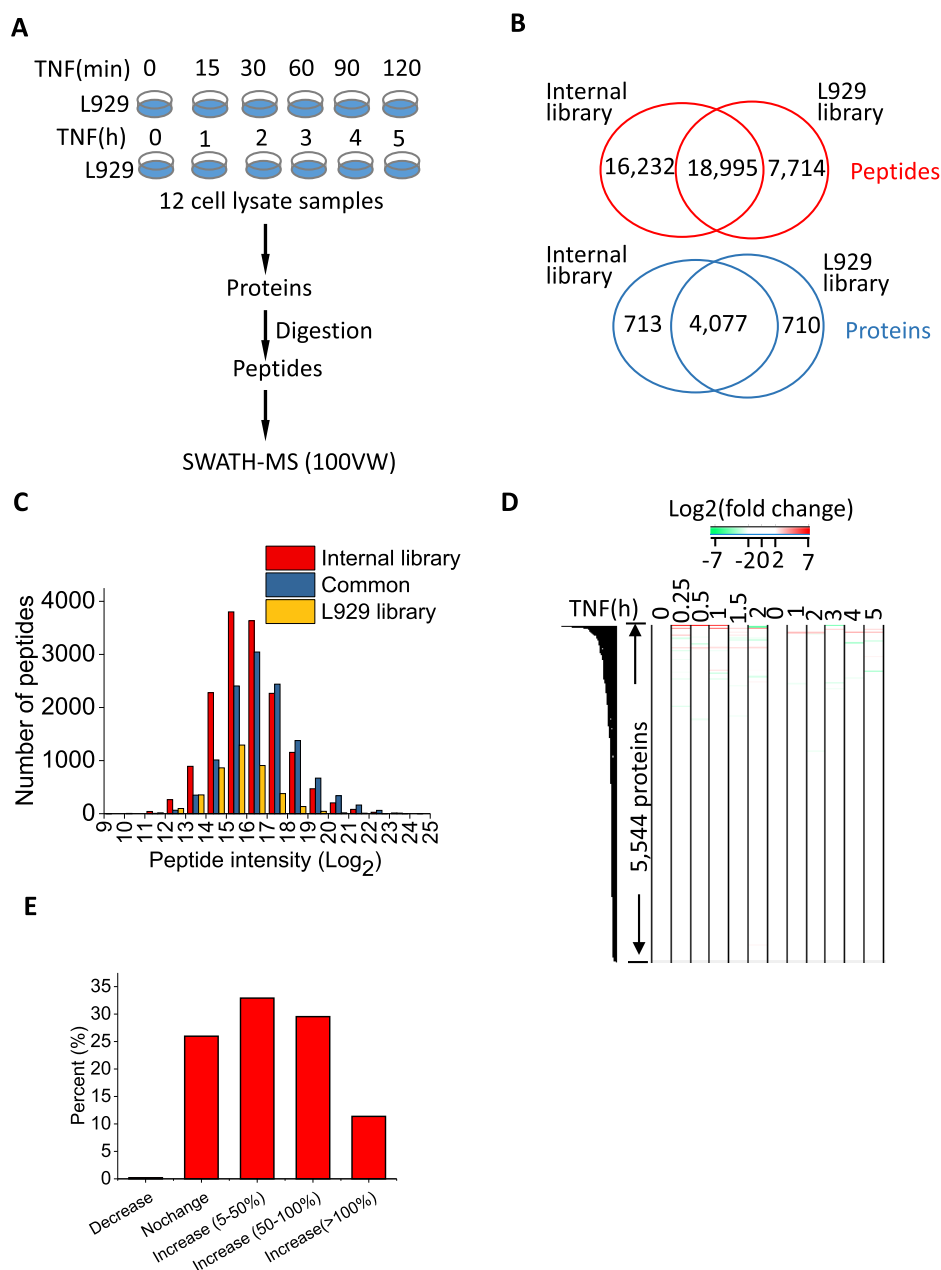


Figure 2. Large number of peptides detected by the internal library were not detected by the L929 library for variable-window SWATH-MS data. (A) Experimental scheme of L929 cells under TNF treatment for various time points. (B) Overlap of quantified peptides or proteins by the internal library and the L929 library at 1% global protein FDR. (C) Intensity distribution of peptides exclusively detected by the internal library or the L929 library or both libraries. (D) Heatmap of quantified protein intensities by the combined library across 12 samples. (E) Percent of proteins with peptide numbers per protein detected by the combined library compared to the L929 library.

of the peptides detected by the L929 library and 66% of the peptides by the internal library (Figure S6C). Importantly, the combined library includes 95.8% of the overlapped peptides of the individual libraries. Thus, the internal library supplements the external library no matter how extensively the external library was generated.

Combination of Internal Library and External Library Largely Extends the Identification Depth for Variable-Window SWATH-MS Data

It was reported that a variable-window setup in SWATH-MS could provide more identified and quantified peptides compared with the fixed-window setup.^{45,46} Thus, we acquired 12 L929 cell lysate samples using SWATH-MS with 100 variable-window

setting (100 VW) (Figure 2A). With OpenSWATH analysis using the L929 library, 4787 proteins were quantified across 12 samples (Table S1). We also employed DIA-Umpire and Group-DIA to build an internal library directly from SWATH-MS data. With this internal library, 4790 proteins were quantified (Table S1). We compared the quantified peptides and proteins (Figure 2B). Remarkably, 44.2% of the total peptides (18 995 of 42 941) were covered by both libraries, and 36.6% (16 621 of 42 941) were detected exclusively by the internal library. At the protein level, 74.1% of the total proteins (4077 of 5500) were identified by both libraries, and 13% (713 of 5500) were exclusively detected by the internal library. The gain in the number of identified proteins by the internal library

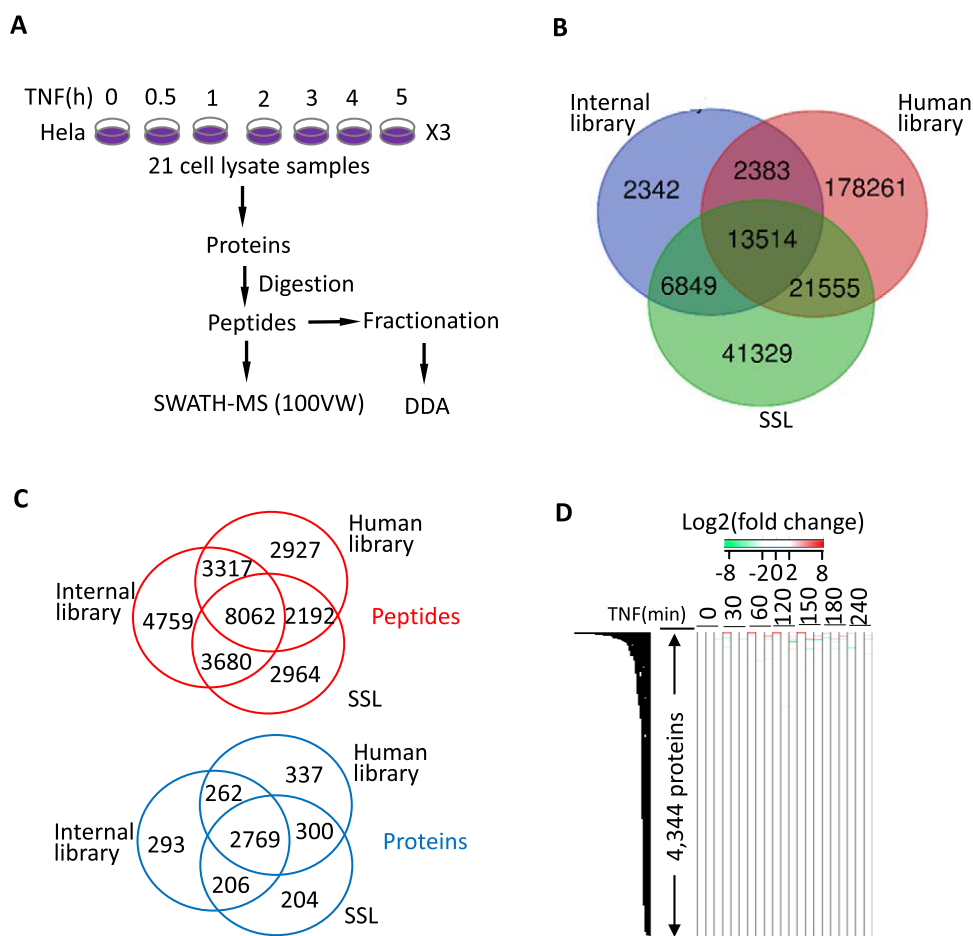


Figure 3. Large number of peptides detected by the internal library were not detected by the external library for 100 VW SWATH-MS data. (A) Experimental scheme of HeLa cells under TNF treatment for various time points. (B) Overlap of peptides in the internal library, SSL, and human library. (C) Overlap of peptides or proteins detected by the three libraries at 1% global protein FDR. (D) Heatmap of quantified protein intensities by the combined library across 12 samples.

was less pronounced compared with that of the peptides, suggesting that most of the extra peptides identified by the internal library belonged to the proteins identified by the L929 library. To investigate the property of these peptides exclusively identified by the internal library, we compared the peptide charges and hydrophobicity. No significant differences in charges and hydrophobicity between the peptides detected by two libraries were observed (Figure S7A,B). We subsequently extracted the peptide intensities. Unexpectedly, while most peptide intensities by the internal library ranged from 14 to 18 at the log₂ scale, the number of peptides identified by the L929 library and common peptides in this intensity range was significantly fewer. These results indicated that the internal library tends to identify low-abundance peptides compared with the L929 library. To enable in-depth interpretation of SWATH-MS data, we combined the L929 library and the internal library. In total, 45 143 peptides that corresponded to 5544 proteins were quantified across 12 samples with the combined library (Figure 2D). Compared with the L929 library, the combined library provided a 61% (16 232 of 26 709) increase in peptide identification and a 15% (713 of 4787) increase in protein identification. In addition, the number of peptides per protein increased in about 70% of the proteins identified by the combined library compared with the L929 library (Figure 2E).

To further demonstrate the advantages of the internal library for analyzing SWATH-MS data from complex samples, we

acquired 21 HeLa cell lysate samples using 100 VW SWATH-MS (Figure 3A). In parallel, we fractionated the peptides derived from the combined 21 samples using SDB-RPS StageTips. The three peptide fractions were analyzed with shotgun MS. DDA runs were subsequently searched, and a consensus spectral library was built (referred to as the sample-specific library, SSL), which consisted of 68 169 peptides and 6308 proteins at 1% protein FDR. We also built an internal library based on 21 SWATH-MS files. The internal library was composed of 3571 proteins and 19 798 peptides. The previously published SWATH-MS spectral library (referred to as the human library hereafter) containing peptide query parameters mapping to 10 000+ human proteins was also used for targeted analysis of HeLa SWATH-MS data. The peptides in three libraries were compared (Figure 3B). Although the human library was generated by combining as many as 331 DDA runs derived from various human samples, a large number of peptides from proteins of HeLa cells (8930 and 46 433 in the internal library and SSL, respectively) were missing in that library. The internal library and SSL were applied to targeted analysis for 21 SWATH-MS runs, resulting in 3530 and 3479 quantified proteins, respectively (Table S2). Next, we used the human library to analyze HeLa SWATH-MS data, which produced 3670 proteins (Table S2). The peptides and proteins identified with three libraries were compared (Figure 3C). Although the overlap of peptide identifications of three libraries was relatively

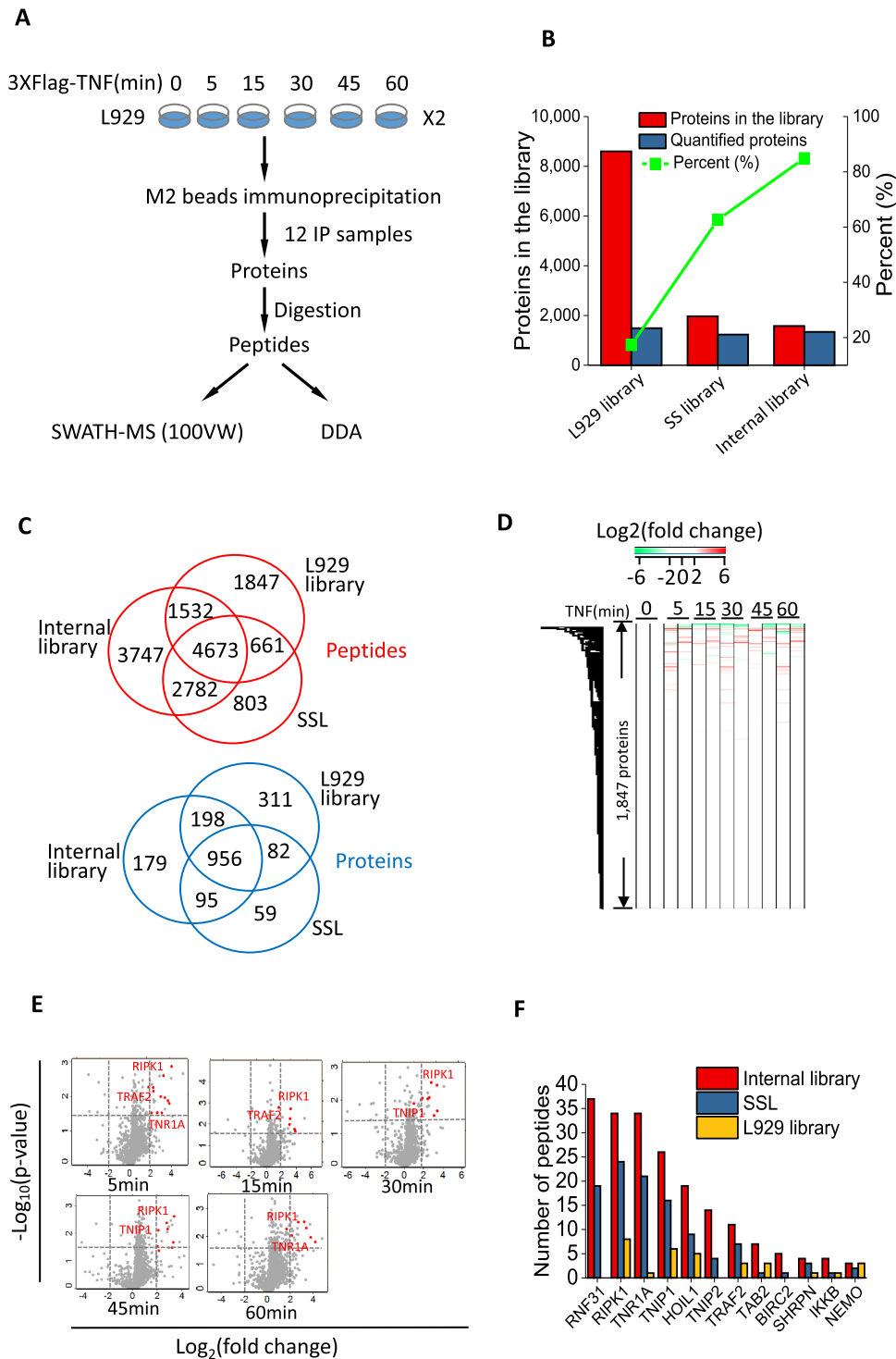


Figure 4. Combination of the internal and the external library enabled in-depth identification of IP SWATH-MS data. (A) Experimental scheme of immunoprecipitation of TNFR1 complexes in L929 cells under TNF treatment for various time points. (B) Comparison of protein numbers in the internal library, the sample-specific library, and the L929 library and protein numbers detected by three libraries. (C) Overlap of peptides or proteins detected by the three libraries at 1% global protein FDR. (D) Heatmap of quantified protein intensities by the combined library across 12 IP samples. (E) Differential expression analysis revealed that some regulated proteins depended on TNF treatment. Several well-known TNFR1 component proteins are labeled in red. (F) The peptide numbers per well-known TNFR1 protein detected by three libraries were compared.

small, the three libraries produced almost 80% identical protein identifications. More importantly, the human library identified the highest number of proteins, while the internal library provided more extra peptide identifications, which is consistent with the case of the L929 study. Compared with SSL, the internal library provided 48% (8076 of 16 878) extra peptide

identifications. Even for the combined peptides from the human library and SSL, the internal library still provided 21% (4759 of 23 142) extra peptide identifications. Next, we combined the three libraries to analyze the SWATH-MS data, which resulted in the quantification of 4344 proteins and 30 780 peptides (Figure 3D and Table S2). Similarly, the peptide number per

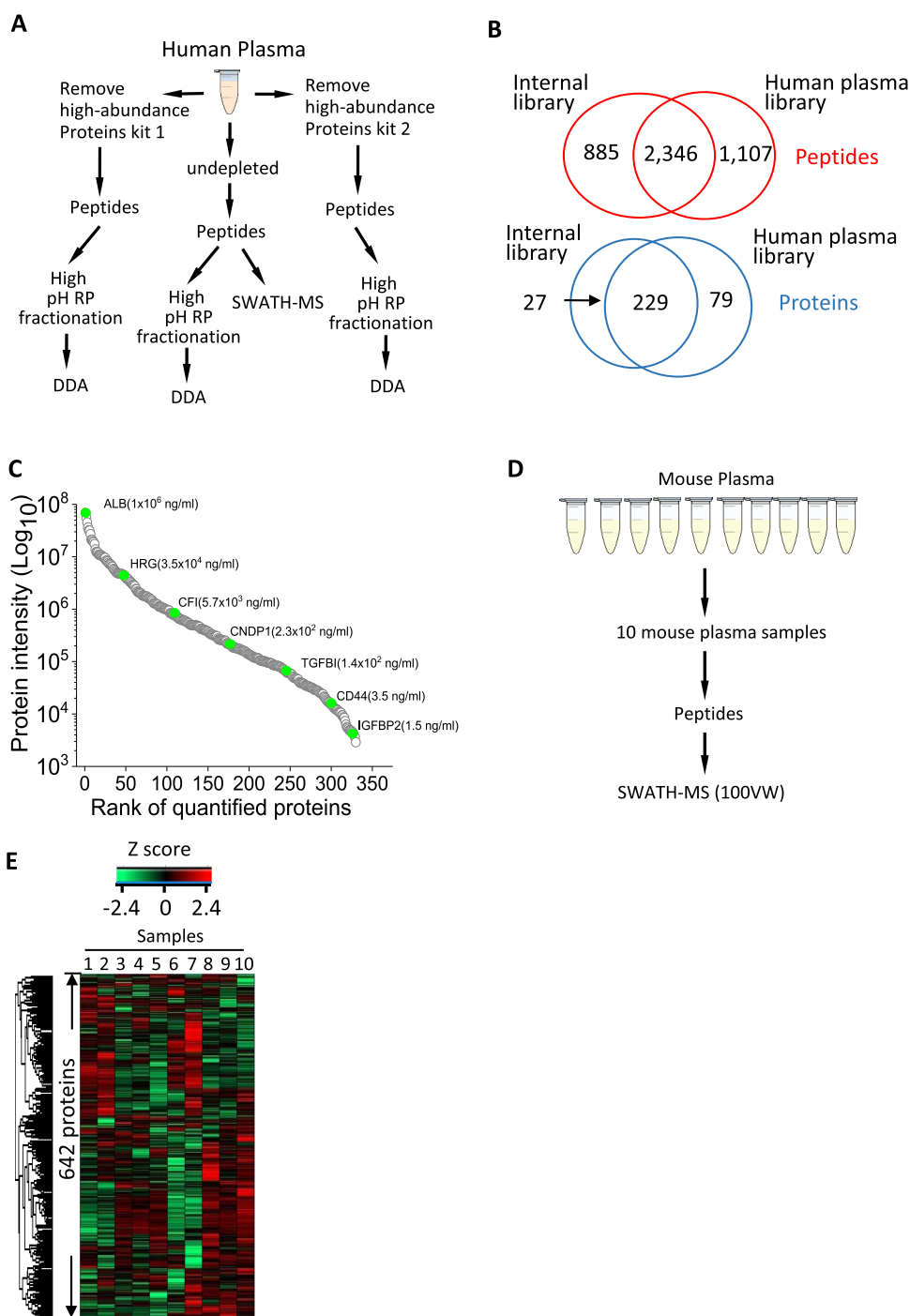


Figure 5. Internal library improves peptide identifications for plasma samples. (A) Building of a deep human plasma spectral library. The undepleted plasma samples and depleted plasma samples were digested and fractionated with high-RP PH liquid chromatography, followed by shotgun MS. (B) Overlap of peptides or proteins detected by the internal library and the human plasma library. (C) Quantitative values of 330 plasma proteins ranked according to their abundance. Several proteins are exemplified labeled in green over the abundance range. (D) Experimental scheme of mouse plasma samples under different treatments. (E) Heatmap of quantified protein intensity using the internal library.

protein of most proteins by the combined library significantly increased compared with SSL (Figure S8A) and the human library (Figure S8B).

In-Depth Exploration of IP SWATH-MS Data through Combining Internal and External Libraries

After the effect of the internal library on the analysis of SWATH-MS data derived from cell lysate samples was investigated, we sought to examine the effect of the internal library on the analysis

of SWATH-MS data of IP, which only contained a small fraction of the total proteome. We used Flag-TNF to treat L929 cells for six time points in biological duplicates and employed anti-Flag beads (M2 beads) to immunoprecipitate tumor necrosis factor receptor 1 (TNFR1) complexes (Figure 4A). Twelve IP samples were analyzed with shotgun MS and 100 VW SWATH-MS. We first used the L929 library to analyze the SWATH-MS data. In total, 1547 proteins were quantified across 12 IP samples (Table S3). Subsequently, we built a sample-specific library (SSL) from

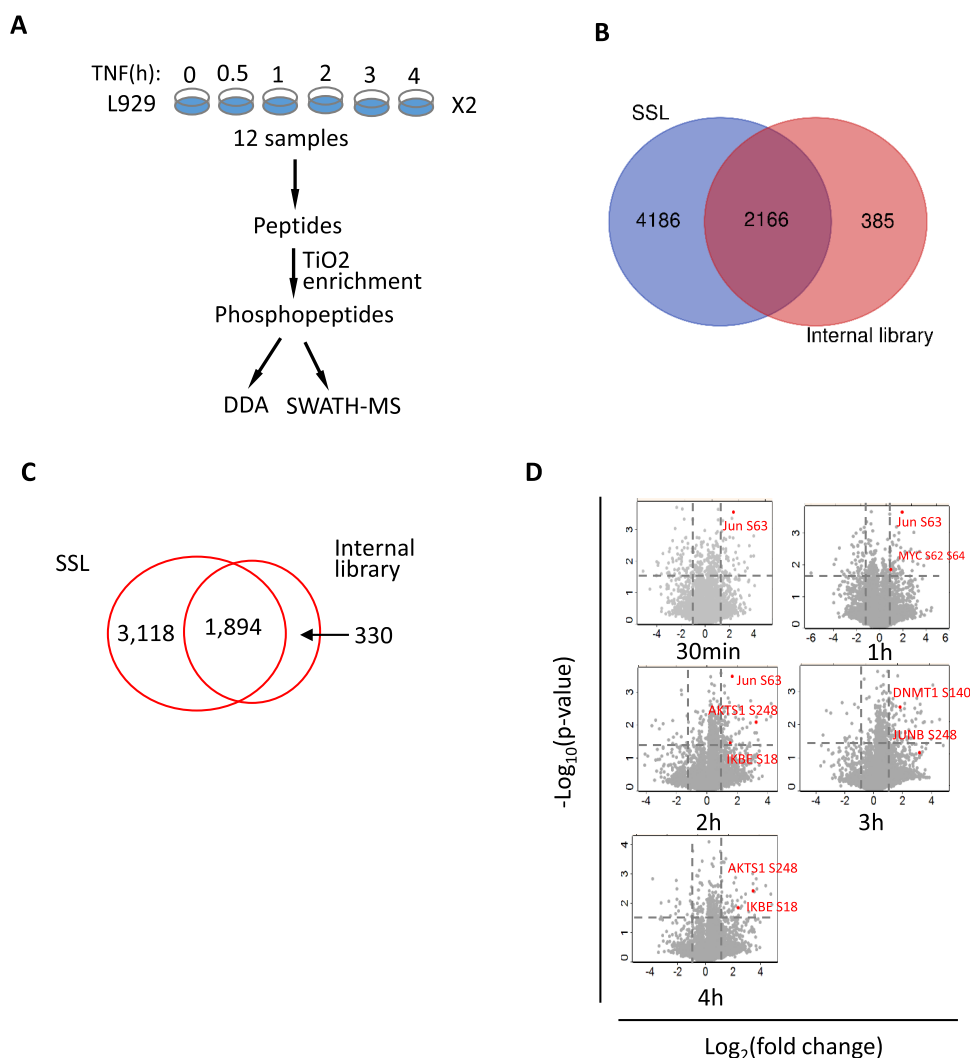


Figure 6. Targeted analysis of phosphoproteomic SWATH-MS data was not benefited from the internal library. (A) Experimental scheme of phosphoproteomics in L929 cells under TNF treatment for various time points. (B) Overlap of phosphopeptides between SSL and the internal library. (C) Overlap of phosphopeptides detected by SSL and the internal library at 1% peptide FDR. (D) Differential expression analysis of regulated phosphopeptides in individual TNF treatment time. The phosphosites that were documented to be regulated in the TNF-treatment way were labeled in red.

DDA runs of IP samples, which was composed of 14 302 peptides and 1968 proteins at 1% protein FDR. The SSL-based analysis resulted in quantification of 1192 proteins (Table S3). Finally, the internal library was applied to analyze these SWATH-MS data. With the internal library, 1428 proteins were quantified (Table S3). The L929-library-based method yielded the highest number of quantified proteins, but the L929 library contained a large number of proteins that did not exist in SWATH-MS data. Remarkably, nearly 90% of proteins in the internal library were detected in SWATH-MS data (Figure 4B). We compared the peptides and proteins identified by the three libraries (Figure 4C). L929-library-based analysis resulted in the highest number of protein identifications, whereas the internal library approach produced most extra peptide identifications. To enable in-depth exploration of IP SWATH-data, we combined these three libraries. The combined library led to the quantification of 1847 proteins and 17 750 peptides (Figure 4D). Differential expression analysis revealed that some proteins were upregulated in the TNFR1 complex (Figure 4E). Some of the upregulated proteins were well-established component proteins of the TNFR1 complex. The peptide numbers of

these proteins identified by the three libraries were compared. The internal-library-based approach was able to identify a dramatically higher number of peptides compared with that based on the L929 library (Figure 4F and Table S3). The internal library also provided a 20–100% increase in the number of identified peptides per protein compared with SSL.

Internal Library Improves the Identification Depth of SWATH-MS Data from Plasma Samples

Plasma proteome is characterized by a vast dynamic range and high complexity, which imposes a serious challenge for deep proteome coverage and biomarker discovery. To explore the effect of the internal library on analysis of SWATH-MS data from plasma samples, we used SWATH-MS to analyze undepleted human plasma samples. First, we generated a deep human plasma library through high-PH reversed-phase fractionation of undepleted and depleted plasma (Figure 5A), which contained 2604 proteins and 20 558 peptides at 1% protein FDR (Table S4). We subsequently acquired two undepleted plasma samples using SWATH-MS in three technical replicates. Targeted analysis of these SWATH-MS

data using the human plasma library resulted in quantification of 308 proteins (Table S4). DIA-Umpire and Group-DIA were used to analyze the SWATH-MS data, and the mgf files generated were employed to build an internal library (Table S4). Targeted analysis using the internal library revealed that 256 proteins were quantified. The peptides and proteins detected by the internal library and the human plasma library were compared, showing that 20% (885 of 4338) of peptides were exclusively detected by the internal library (Figure 5B). The library merged with the internal library and the human plasma library identified 330 proteins (Figure 5C and Table S4). The lowest protein abundance in human plasma detected by SWATH-MS is about 1–10 ng/mL (Figure 5C).

In addition, we acquired 10 undepleted mouse plasma samples using SWATH-MS (Figure 5D). The internal library was used for targeted analysis of these SWATH-MS data, resulting in quantification of 642 proteins and 7007 peptides across 10 mouse plasma samples (Figure 5E and Table S4). The dynamic range of the intensities of quantified proteins was about 10^5 (Figure S9). We compared the identified proteins with mouse plasma proteins that were available at www.peptideatlas.org and found 50% of them were overlapped (Figure S10).

Internal Library Did Not Benefit Phosphopeptide Detection from Phosphoproteomic SWATH-MS Data

To further investigate whether analysis of phosphoproteomic SWATH-MS data benefits from the internal library, we acquired 12 phosphoproteomic samples using SWATH-MS (Figure 6A). Twelve DDA runs were searched, resulting in 7,687 phosphopeptides at 1% peptide FDR (Table S5). The phosphopeptide enrichment efficiency is 95.9% (7687 of total 8012), and localized phosphopeptides are 6773 (PTMprophet probability ≥ 0.7) (Figure S12). These localized phosphopeptides were constructed as the sample-specific library (SSL). Twelve SWATH-MS runs were analyzed by Group-DIA and DIA-Umpire, and the generated mgf files were searched, which resulted in 2719 localized phosphopeptides (Figure S11 and Table S5). These localized phosphopeptides were built as an internal library. The phosphopeptides were compared between SSL and the internal library. SSL covered 85% phosphopeptides of the internal library (Figure 6B). These libraries were used for targeted analysis of SWATH-MS data. In total, 5292 phosphopeptides were quantified across 12 samples using SSL, while 2371 phosphopeptides were quantified using the internal library (Table S5). Phosphopeptides from SSL covered 85% of that from the internal library (Figure 6C). Intensities of phosphopeptides between the two samples were compared, showing that there was good reproducibility for phosphoproteomic SWATH-MS data (Figure S12). Differential expression analysis revealed that many phosphopeptides were upregulated in L929 cells under TNF treatment, among which some were well-established TNF-induced phosphosites (Figure 6D).

DISCUSSION

Targeted analysis of SWATH-MS data is almost entirely dependent on the spectral library, which includes the external library and the internal library. The external libraries can be divided into the sample-specific spectral library (SSL) and the extensive spectral library. The former is constructed by shotgun MS analysis of the specific samples that are subjected to SWATH-MS analysis, whereas the latter is typically referred to as the species-specific spectral library that is generated through extensive fractionation of protein or peptides. However, the

internal library is built on DDA-like files directly generated from SWATH-MS. Targeted analysis of SWATH-MS in most research is usually performed by use of the external library. In this study, we investigated the effect of the internal library on the targeted analysis of SWATH-MS from various kinds of samples.

First, we generated a comprehensive external spectral library of the murine L929 cell line. We acquired L929 cell lysate samples using SWATH-MS. Two SWATH-MS settings were adopted in this study. One has fixed width of 25 Da with 32 windows, and the other has variable width with 100 windows, where the minimum window is about 5 Da. Much less precursor ions were isolated in one Q1 window in variable windows, leading to significantly fewer interference product ions in one MS2 scan. Therefore, specificity and sensitivity of XICs of product ions can be largely improved, which resulted in better match of precursor–product pairs in DIA-Umpire or Group-DIA software. As expected, the internal library from SWATH-MS with variable windows identified much more peptides than that with fixed windows. More importantly, a large fraction of peptides (38%, 16 232 of 42 941) by the internal library cannot be detected in the L929 library for 100 VW SWATH-MS data. This result suggested that the L929 library is not complete at the peptide level for L929 SWATH-MS data. Similarly, the extensive human library only yielded 59% (16 498 of 27 901) of the total peptides for SWATH-MS from HeLa lysate samples. In contrast, 71% (19 818 of 27 901) of the total peptides were detected by the internal library alone. Indeed, the combined peptides from SSL and the internal library already accounted for 90% (24 974 of 27 901) of the total peptides for HeLa SWATH-MS data (Figure 3C). These results suggested that the comprehensive external spectral library is probably incomplete at the peptide level for SWATH-MS from complex samples, such as cell lysate and tissues.

We next investigated the effect of the internal library on the analysis of SWATH-MS from IP samples, which are less complex than cell lysate samples. IP experiments were conducted in L929 cells. In this case, the internal library contributed to 80% (12 734 of 16 045) of the total peptides, while the L929 library produced 54% (8713 of 16 045) of the total peptides. Similarly, the combined peptides from SSL and the internal library already made up 88% (14 198 of 16 045) of the total peptides. For SWATH-MS data from the human plasma samples, the internal library still produced 25% (885 of 3453) of the extra peptides compared with the extensive external library.

Finally, we evaluated the influence of the internal library on analyzing SWATH-MS from phosphoproteomic samples. The internal library identified significantly fewer phosphopeptides than SSL, and the phosphopeptides from the internal library were almost covered by those from SSL. The result showed that SSL is efficient for analysis of phosphoproteomic SWATH-MS data. The poor performance of the internal library on phosphoproteomic SWATH-MS is probably due to low intensities of phosphopeptides,⁴⁷ which hampers precursor–product ion matching in pseudo-spectra file generating software.

The DIA-Umpire papers published in Nature Methods of 2015 proposed the notion of the internal library, which is directly generated from DIA files.²⁰ The Proteomics papers in 2016 described an improved version of DIA-Umpire, which can be applied to DIA data acquired on Orbitrap instrument.⁴⁸ They compared the identifications of the internal libraries and project-specific libraries as well as library-based quantitative results of targeted DIA analysis using DIA-Umpire. However, they did not compare the results of targeted DIA analysis using the internal

spectral libraries and those using public source libraries with the stringent FDR cutoff at the protein level. Besides, no library combination procedures were performed in the papers. Furthermore, the data set presented in the two studies is relatively small. The study in Nature Biotechnology compared performance of four library-based software as well as DIA-Umpire in analyzing SWATH-MS data.²⁴ The authors mainly focused on the highly convergent results obtained by the five software, demonstrating their robustness of DIA-based label-free quantitative proteomics. Similar to DIA-Umpire papers, the authors used the project-specific libraries or internal libraries, instead of the public source library, to analyze the SWATH-MS data. They did not perform any library combination. When comparing the quantitative results obtained from different software, FDR estimate strategies used in different tools may have introduced the identification bias. The very recent study from the Spectronaut team published in Molecular Omics⁴⁹ described the use of library combination in analyzing DIA data, supporting that the combined library provides an improved result. The details regarding FDR estimation in Spectronaut were unavailable in all manuscripts. In contrast, OpenSWATH, PyProphet, and TRIC, which are latest and sophisticated open-source tools and have successfully been employed in large-scale DIA data,^{41,50} are utilized in our study. It is much easier to reproduce the results obtained by the open-source tools compared with those obtained by the commercial ones. Collectively, our study presents a comprehensive and strict comparison of different libraries in analyzing a variety of DIA data and shows the improved performance of the combined library.

In addition, our SWATH-MS-based qualitative proteomics reveals the biological implications for the TNF-signaling pathway. We examined the quantitative protein intensities in the 100-VW L929 data set. TNF stimulation is known to activate the NF- κ B pathway, leading to production of a variety of proteins including cytokines and chemokines. We compared the protein intensities at 3 h to those at 0 h and used a ratio of 3 as the upregulation cutoff. Eighty-seven proteins were found to be upregulated (Table S1), of which several TNF-induced cytokines and chemokines such as CCL2, TNF, CCL7, and CXCL1 were found. Besides, JUNB, MAPK9, and MAP2K7, which are involved in the TNF-signaling pathway, also exist in the upregulation list. We clustered the biological pathways of these 87 proteins and found the top1 pathway is the TNF pathway (Figure S13A). For the HeLa data set, we extracted TNF-induced proteins at TNF 180 min treatment ($\log_2(\text{fold change}) > 1$ and $-\log_{10}(p\text{-value}) > 1.5$) (Figure S13B). From these upregulated proteins, we did not observe the TNF-induced cytokines or chemokines, as detected in the TNF-treated L929 cells. However, JUNB and NF κ B2, which are the proteins targeted by NF- κ B, are in the TNF-induced protein list. These results could be attributed to the different mechanism of two cells in response to TNF treatment, but we cannot rule out the possibility that less coverage of HeLa proteome relative to that of L929 cells (5544 proteins vs 4344 proteins) results in the phenomena.

In the L929 phosphoproteomics data set, phosphorylation of Serine 63 on Jun and Serine 11 on TRAF2 showed significant upregulation upon TNF stimulation (Figure 6D). S63 of Jun was reported to be phosphorylated by JNK2,^{51,52} which was activated by TNF stimulation. Phosphorylation of S11 on TRAF2, which was phosphorylated by IKKi,⁵³ was essential for TNF-induced secondary IKK activation.⁵⁴

In our experiment, Flag-TNF was used to treat L929 cells, and Flag-TNF can bind to TNFR1 (tumor necrosis factor receptor 1) and form a compact complex. Flag-TNF is also frequently employed in the purification of the TNFR1 complex in other studies.^{55–59} From the differential expression analysis (Figure 4E), we selected all TNF-induced proteins in TNF IP experiments and plotted dynamic change curves. Almost all of them are well-established TNFR1 interacting proteins.⁶⁰ As shown in Figure S14, different proteins are recruited to TNFR1 at different TNF stimulation times. TRADD and RIP1 are recruited to TNFR1 at 5 min and dissociated from the complex after 15 min, whereas TRAF2 is recruited to TNFR1 and remains unchanged over treatment time. A20 is recruited to TNFR1 at 60 min, but TNIP2, an A20 interacting protein, apparently shows a distinct pattern with A20. Overall, these different patterns by which proteins are recruited to the TNFR1 complex are probably tightly connected to their functions in the TNF pathway.

In summary, the internal library yielded a large number of peptides that cannot be detected by the external library for SWATH-MS data from immunoprecipitations, cell lysates, and plasmas. The internal library has no significant benefits on phosphoproteomic SWATH-MS data. In nonphosphoproteomic SWATH-MS data, the peptides exclusively detected by the internal library should not be ignored. Therefore, the internal library is highly recommended to be incorporated into the external library, which can improve identification depth on the peptide level without extra peptide samples and additional instrument measurement time.

■ ASSOCIATED CONTENT

Supporting Information

The Supporting Information is available free of charge on the ACS Publications website at DOI: 10.1021/acs.jproteome.9b00669.

Overview of generation of the spectral library of whole proteome of the murine L929 cell line (Figure S1); quantified proteins in the L929 fixed-window SWATH-MS data set (Figure S2); Pearson correlation of protein or peptide intensities identified in two samples using the L929 library or the internal library (Figure S3); comparison of properties of identified peptide precursors using the L929 library or the internal library (Figure S4); XICs of six product ions used for quantification for several common peptides from two libraries (Figure S5); CVs of quantified proteins using the combined library and comparisons of identified proteins and peptides using the combined library, internal library, or L929 library (Figure S6); comparison of charges or hydrophobicity of peptides detected by the L929 library or the internal library (Figure S7); percent of detected peptides per protein with a combined library compared with the SSL or human library (Figure S8); quantitative values of mouse plasma proteins ranked according to their abundance (Figure S9); overlap of mouse plasma proteins detected by the internal library and mouse plasma proteins in PeptideAtlas (Figure S10); numbers of peptides identified by DDA or pseudo-spectra files in phosphoproteomic SWATH-MS data (Figure S11); Pearson correlation of phosphopeptide intensities identified in two samples using the DDA library (Figure S12); analysis of biological pathways in which TNF-induced proteins are involved in

L929 cells and differential expression analysis of quantitative proteins in TNF-treated HeLa cells (Figure S13); temporal profiles of upregulated proteins in the TNFR1 IP data set (Figure S14); validation of confidence of peptides and proteins in the combined library (Figure S15) (PDF)

Peptides and proteins in the L929 data set (Table S1); peptides and proteins in the HeLa data set (Table S2); peptides and proteins in the TNFR1 IP data set (Table S3); peptides and proteins in the plasma data set (Table S4); phosphopeptides in the phosphoproteomics data set (Table S5) (ZIP)

AUTHOR INFORMATION

Corresponding Authors

*E-mail: zhongcq@xmu.edu.cn (C.-Q.Z.).

*E-mail: jhan@xmu.edu.cn (J.H.).

ORCID

Chuan-Qi Zhong: 0000-0002-8354-7727

Notes

The authors declare no competing financial interest.

ACKNOWLEDGMENTS

This work was supported by the National Natural Science Foundation of China (81788101), National Basic Research Program of China (973 Program 2015CB553800), the National Natural Science Foundation of China (31420103910 and 81630042), the 111 Project (B12001), the Young Scientists Fund of the National Natural Science Foundation of China (31601115), and the National Science Foundation of China for Fostering Talents in Basic Research (J1310027). We thank Drs. Zhuobin Xu and Yuwei Yu for help in using the high-performance computer. We thank Dr. Wei Han for discussions on sample preparation.

REFERENCES

- (1) Aebersold, R.; Mann, M. Mass-spectrometric exploration of proteome structure and function. *Nature* **2016**, *537*, 347–355.
- (2) Anderson, L.; Hunter, C. L. Quantitative mass spectrometry multiple reaction monitoring assays for major plasma proteins. *Mol. Cell. Proteomics* **2006**, *5*, 573–588.
- (3) Kuhn, E.; Wu, J.; Karl, J.; Liao, H.; Zolg, W.; Guild, B. Quantification of C-reactive protein in the serum of patients with rheumatoid arthritis using multiple reaction monitoring mass spectrometry and ¹³C-labeled peptide standards. *Proteomics* **2004**, *4*, 1175–1186.
- (4) Gallien, S.; Duriez, E.; Demeure, K.; Domon, B. Selectivity of LC-MS/MS analysis: implication for proteomics experiments. *J. Proteomics* **2013**, *81*, 148–158.
- (5) Venable, J. D.; Dong, M. Q.; Wohlschlegel, J.; Dillin, A.; Yates, J. R. Automated approach for quantitative analysis of complex peptide mixtures from tandem mass spectra. *Nat. Methods* **2004**, *1*, 39–45.
- (6) Panchoaud, A.; Scherl, A.; Shaffer, S. A.; von Haller, P. D.; Kulasekara, H. D.; Miller, S. L.; Goodlett, D. R. Precursor acquisition independent from ion count: how to dive deeper into the proteomics ocean. *Anal. Chem.* **2009**, *81*, 6481–6488.
- (7) Plumb, R. S.; Johnson, K. A.; Rainville, P.; Smith, B. W.; Wilson, I. D.; Castro-Perez, J. M.; Nicholson, J. K. UPLC/MS(E): a new approach for generating molecular fragment information for biomarker structure elucidation. *Rapid Commun. Mass Spectrom.* **2006**, *20*, 1989–1994.

- (8) Purvine, S.; Eppel, J. T.; Yi, E. C.; Goodlett, D. R. Shotgun collision-induced dissociation of peptides using a time of flight mass analyzer. *Proteomics* **2003**, *3*, 847–850.

- (9) Bilbao, A.; Varesio, E.; Luban, J.; Strambio-De-Castilla, C.; Hopfgartner, G.; Muller, M.; Lisacek, F. Processing strategies and software solutions for data-independent acquisition in mass spectrometry. *Proteomics* **2015**, *15*, 964–980.

- (10) Gillet, L. C.; Navarro, P.; Tate, S.; Rost, H.; Selevsek, N.; Reiter, L.; Bonner, R.; Aebersold, R. Targeted data extraction of the MS/MS spectra generated by data-independent acquisition: a new concept for consistent and accurate proteome analysis. *Mol. Cell. Proteomics* **2012**, *11*, No. O111.016717.

- (11) Zi, J.; Zhang, S.; Zhou, R.; Zhou, B.; Xu, S.; Hou, G.; Tan, F.; Wen, B.; Wang, Q.; Lin, L.; Liu, S. Expansion of the ion library for mining SWATH-MS data through fractionation proteomics. *Anal. Chem.* **2014**, *86*, 7242–7246.

- (12) Parker, S. J.; Venkatraman, V.; Van Eyk, J. E. Effect of peptide assay library size and composition in targeted data-independent acquisition-MS analyses. *Proteomics* **2016**, *16*, 2221–2237.

- (13) Wu, J. X.; Song, X.; Pascovici, D.; Zaw, T.; Care, N.; Krisp, C.; Molloy, M. P. SWATH Mass Spectrometry Performance Using Extended Peptide MS/MS Assay Libraries. *Mol. Cell. Proteomics* **2016**, *15*, 2501–2514.

- (14) Govaert, E.; Van Steendam, K.; Willems, S.; Vossaert, L.; Dhaenens, M.; Deforce, D. Comparison of fractionation proteomics for local SWATH library building. *Proteomics* **2017**, *17*, 15–16.

- (15) Rosenberger, G.; Koh, C. C.; Guo, T.; Rost, H. L.; Kouvonen, P.; Collins, B. C.; Heusel, M.; Liu, Y.; Caron, E.; Vichalkovski, A.; Faini, M.; Schubert, O. T.; Faridi, P.; Ebhardt, H. A.; Matondo, M.; Lam, H.; Bader, S. L.; Campbell, D. S.; Deutsch, E. W.; Moritz, R. L.; Tate, S.; Aebersold, R. A repository of assays to quantify 10,000 human proteins by SWATH-MS. *Sci. Data* **2014**, *1*, No. 140031.

- (16) Picotti, P.; Clement-Ziza, M.; Lam, H.; Campbell, D. S.; Schmidt, A.; Deutsch, E. W.; Rost, H.; Sun, Z.; Rinner, O.; Reiter, L.; Shen, Q.; Michaelson, J. J.; Frei, A.; Alberti, S.; Kusebauch, U.; Wollscheid, B.; Moritz, R. L.; Beyrer, A.; Aebersold, R. A complete mass-spectrometric map of the yeast proteome applied to quantitative trait analysis. *Nature* **2013**, *494*, 266–270.

- (17) Schubert, O. T.; Ludwig, C.; Kogadeeva, M.; Zimmermann, M.; Rosenberger, G.; Gengenbacher, M.; Gillet, L. C.; Collins, B. C.; Rost, H. L.; Kaufmann, S. H.; Sauer, U.; Aebersold, R. Absolute Proteome Composition and Dynamics during Dormancy and Resuscitation of *Mycobacterium tuberculosis*. *Cell Host Microbe* **2015**, *18*, 96–108.

- (18) Caron, E.; Espona, L.; Kowalewski, D. J.; Schuster, H.; Termette, N.; Alpizar, A.; Schittenhelm, R. B.; Ramarathinam, S. H.; Lindestam Arlehamn, C. S.; Chiek Koh, C.; Gillet, L. C.; Rabsteyn, A.; Navarro, P.; Kim, S.; Lam, H.; Sturm, T.; Marcilla, M.; Sette, A.; Campbell, D. S.; Deutsch, E. W.; Moritz, R. L.; Purcell, A. W.; Rammensee, H. G.; Stevanovic, S.; Aebersold, R. An open-source computational and data resource to analyze digital maps of immunopeptidomes. *Elife* **2015**, *4*, No. e07661.

- (19) Kusebauch, U.; Campbell, D. S.; Deutsch, E. W.; Chu, C. S.; Spicer, D. A.; Brusniak, M. Y.; Slagel, J.; Sun, Z.; Stevens, J.; Grimes, B.; Shteynberg, D.; Hoopmann, M. R.; Blattmann, P.; Ratushny, A. V.; Rinner, O.; Picotti, P.; Carapito, C.; Huang, C. Y.; Kapousouz, M.; Lam, H.; Tran, T.; Demir, E.; Aitchison, J. D.; Sander, C.; Hood, L.; Aebersold, R.; Moritz, R. L. Human SRMATlas: A Resource of Targeted Assays to Quantify the Complete Human Proteome. *Cell* **2016**, *166*, 766–778.

- (20) Tsou, C. C.; Avtonomov, D.; Larsen, B.; Tucholska, M.; Choi, H.; Gingras, A. C.; Nesvizhskii, A. I. DIA-Umpire: comprehensive computational framework for data-independent acquisition proteomics. *Nat. Methods* **2015**, *12*, 258–264 7 p following 264.

- (21) Li, Y.; Zhong, C. Q.; Xu, X.; Cai, S.; Wu, X.; Zhang, Y.; Chen, J.; Shi, J.; Lin, S.; Han, J. Group-DIA: analyzing multiple data-independent acquisition mass spectrometry data files. *Nat. Methods* **2015**, *12*, 1105–1106.

- (22) Ting, Y. S.; Egertson, J. D.; Bollinger, J. G.; Searle, B. C.; Payne, S. H.; Noble, W. S.; MacCoss, M. J. PECAN: library-free peptide

detection for data-independent acquisition tandem mass spectrometry data. *Nat. Methods* **2017**, *14*, 903–908.

(23) Wang, J.; Tucholska, M.; Knight, J. D.; Lambert, J. P.; Tate, S.; Larsen, B.; Gingras, A. C.; Bandeira, N. MSPLIT-DIA: sensitive peptide identification for data-independent acquisition. *Nat. Methods* **2015**, *12*, 1106–1108.

(24) Navarro, P.; Kuharev, J.; Gillet, L. C.; Bernhardt, O. M.; MacLean, B.; Rost, H. L.; Tate, S. A.; Tsou, C. C.; Reiter, L.; Distler, U.; Rosenberger, G.; Perez-Riverol, Y.; Nesvizhskii, A. I.; Aebersold, R.; Tenzer, S. A multicenter study benchmarks software tools for label-free proteome quantification. *Nat. Biotechnol.* **2016**, *34*, 1130–1136.

(25) Humphrey, S. J.; Karayel, O.; James, D. E.; Mann, M. High-throughput and high-sensitivity phosphoproteomics with the EasyPhos platform. *Nat. Protoc.* **2018**, *13*, 1897–1916.

(26) Meier, F.; Brunner, A. D.; Koch, S.; Koch, H.; Lubeck, M.; Krause, M.; Goedecke, N.; Decker, J.; Kosinski, T.; Park, M. A.; Bache, N.; Hoerning, O.; Cox, J.; Rather, O.; Mann, M. Online Parallel Accumulation-Serial Fragmentation (PASEF) with a Novel Trapped Ion Mobility Mass Spectrometer. *Mol. Cell. Proteomics* **2018**, *17*, 2534–2545.

(27) Meier, F.; Beck, S.; Grassl, N.; Lubeck, M.; Park, M. A.; Raether, O.; Mann, M. Parallel Accumulation-Serial Fragmentation (PASEF): Multiplying Sequencing Speed and Sensitivity by Synchronized Scans in a Trapped Ion Mobility Device. *J. Proteome Res.* **2015**, *14*, 5378–5387.

(28) Chambers, M. C.; Maclean, B.; Burke, R.; Amodei, D.; Ruderman, D. L.; Neumann, S.; Gatto, L.; Fischer, B.; Pratt, B.; Egerton, J.; Hoff, K.; Kessner, D.; Tasman, N.; Shulman, N.; Frewen, B.; Baker, T. A.; Brusniak, M. Y.; Paulse, C.; Creasy, D.; Flashner, L.; Kani, K.; Moulding, C.; Seymour, S. L.; Nuwaysir, L. M.; Lefebvre, B.; Kuhlmann, F.; Roark, J.; Rainer, P.; Detlev, S.; Hemenway, T.; Huhmer, A.; Langridge, J.; Connolly, B.; Chadick, T.; Holly, K.; Eckels, J.; Deutsch, E. W.; Moritz, R. L.; Katz, J. E.; Agus, D. B.; MacCoss, M.; Tabb, D. L.; Mallick, P. A cross-platform toolkit for mass spectrometry and proteomics. *Nat. Biotechnol.* **2012**, *30*, 918–920.

(29) Deutsch, E. W.; Mendoza, L.; Shteynberg, D.; Farrah, T.; Lam, H.; Tasman, N.; Sun, Z.; Nilsson, E.; Pratt, B.; Prazan, B.; Eng, J. K.; Martin, D. B.; Nesvizhskii, A. I.; Aebersold, R. A guided tour of the Trans-Proteomic Pipeline. *Proteomics* **2010**, *10*, 1150–1159.

(30) Eng, J. K.; Jahan, T. A.; Hoopmann, M. R. Comet: an open-source MS/MS sequence database search tool. *Proteomics* **2013**, *13*, 22–24.

(31) Craig, R.; Beavis, R. C. TANDEM: matching proteins with tandem mass spectra. *Bioinformatics* **2004**, *20*, 1466–1467.

(32) Ma, K.; Vitek, O.; Nesvizhskii, A. I. A statistical model-building perspective to identification of MS/MS spectra with PeptideProphet. *BMC Bioinf.* **2012**, *13*, S1.

(33) Shteynberg, D.; Deutsch, E. W.; Lam, H.; Eng, J. K.; Sun, Z.; Tasman, N.; Mendoza, L.; Moritz, R. L.; Aebersold, R.; Nesvizhskii, A. I. iProphet: multi-level integrative analysis of shotgun proteomic data improves peptide and protein identification rates and error estimates. *Mol. Cell. Proteomics* **2011**, *10*, No. M111.007690.

(34) Reiter, L.; Claassen, M.; Schrimpf, S. P.; Jovanovic, M.; Schmidt, A.; Buhmann, J. M.; Hengartner, M. O.; Aebersold, R. Protein identification false discovery rates for very large proteomics data sets generated by tandem mass spectrometry. *Mol. Cell. Proteomics* **2009**, *8*, 2405–2417.

(35) Nesvizhskii, A. I.; Keller, A.; Kolker, E.; Aebersold, R. A statistical model for identifying proteins by tandem mass spectrometry. *Anal. Chem.* **2003**, *75*, 4646–4658.

(36) Lam, H.; Deutsch, E. W.; Eddes, J. S.; Eng, J. K.; Stein, S. E.; Aebersold, R. Building consensus spectral libraries for peptide identification in proteomics. *Nat. Methods* **2008**, *5*, 873–875.

(37) Röst, H. L.; Sachsenberg, T.; Aiche, S.; Bielow, C.; Weisser, H.; Aicheler, F.; Andreotti, S.; Ehrlich, H. C.; Gutenbrunner, P.; Kenar, E.; Liang, X.; Nahnsen, S.; Nilse, L.; Pfeuffer, J.; Rosenberger, G.; Rurik, M.; Schmitt, U.; Veit, J.; Walzer, M.; Wojnar, D.; Wolski, W. E.; Schilling, O.; Choudhary, J. S.; Malmstrom, L.; Aebersold, R.; Reinert,

K.; Kohlbacher, O. OpenMS: a flexible open-source software platform for mass spectrometry data analysis. *Nat. Methods* **2016**, *13*, 741–748.

(38) Parker, S. J.; Rost, H.; Rosenberger, G.; Collins, B. C.; Malmstrom, L.; Amodei, D.; Venkatraman, V.; Raedschelders, K.; Van Eyk, J. E.; Aebersold, R. Identification of a Set of Conserved Eukaryotic Internal Retention Time Standards for Data-independent Acquisition Mass Spectrometry. *Mol. Cell. Proteomics* **2015**, *14*, 2800–2813.

(39) Escher, C.; Reiter, L.; MacLean, B.; Ossola, R.; Herzog, F.; Chilton, J.; MacCoss, M. J.; Rinner, O. Using iRT, a normalized retention time for more targeted measurement of peptides. *Proteomics* **2012**, *12*, 1111–1121.

(40) Reiter, L.; Rinner, O.; Picotti, P.; Huttenhain, R.; Beck, M.; Brusniak, M. Y.; Hengartner, M. O.; Aebersold, R. mProphet: automated data processing and statistical validation for large-scale SRM experiments. *Nat. Methods* **2011**, *8*, 430–435.

(41) Rosenberger, G.; Bludau, I.; Schmitt, U.; Heusel, M.; Hunter, C. L.; Liu, Y.; MacCoss, M. J.; MacLean, B. X.; Nesvizhskii, A. I.; Pedrioli, P. G. A.; Reiter, L.; Rost, H. L.; Tate, S.; Ting, Y. S.; Collins, B. C.; Aebersold, R. Statistical control of peptide and protein error rates in large-scale targeted data-independent acquisition analyses. *Nat. Methods* **2017**, *14*, 921–927.

(42) Röst, H. L.; Liu, Y.; D'Agostino, G.; Zanella, M.; Navarro, P.; Rosenberger, G.; Collins, B. C.; Gillet, L.; Testa, G.; Malmström, L.; Aebersold, R. TRIC: an automated alignment strategy for reproducible protein quantification in targeted proteomics. *Nat. Methods* **2016**, *13*, 777–783.

(43) Muntel, J.; Xuan, Y.; Berger, S. T.; Reiter, L.; Bachur, R.; Kentsis, A.; Steen, H. Advancing Urinary Protein Biomarker Discovery by Data-Independent Acquisition on a Quadrupole-Orbitrap Mass Spectrometer. *J. Proteome Res.* **2015**, *14*, 4752–4762.

(44) Röst, H. L.; Rosenberger, G.; Navarro, P.; Gillet, L.; Miladinović, S. M.; Schubert, O. T.; Wolski, W.; Collins, B. C.; Malmström, J.; Malmström, L.; Aebersold, R. OpenSWATH enables automated, targeted analysis of data-independent acquisition MS data. *Nat. Biotechnol.* **2014**, *32*, 219–223.

(45) Zhang, Y.; Bilbao, A.; Bruderer, T.; Luban, J.; Strambio-De-Castilla, C.; Lisacek, F.; Hopfgartner, G.; Varesio, E. The Use of Variable Q1 Isolation Windows Improves Selectivity in LC-SWATH-MS Acquisition. *J. Proteome Res.* **2015**, *14*, 4359–4371.

(46) Li, S.; Cao, Q.; Xiao, W.; Guo, Y.; Yang, Y.; Duan, X.; Shui, W. Optimization of Acquisition and Data-Processing Parameters for Improved Proteomic Quantification by Sequential Window Acquisition of All Theoretical Fragment Ion Mass Spectrometry. *J. Proteome Res.* **2017**, *16*, 738–747.

(47) Dreier, R. F.; Ahrne, E.; Broz, P.; Schmidt, A. Global Ion Suppression Limits the Potential of Mass Spectrometry Based Phosphoproteomics. *J. Proteome Res.* **2019**, *18*, 493–507.

(48) Tsou, C. C.; Tsai, C. F.; Teo, G. C.; Chen, Y. J.; Nesvizhskii, A. I. Untargeted, spectral library-free analysis of data-independent acquisition proteomics data generated using Orbitrap mass spectrometers. *Proteomics* **2016**, *16*, 2257–2271.

(49) Muntel, J.; Gandhi, T.; Verbeke, L.; Bernhardt, O. M.; Treiber, T.; Bruderer, R.; Reiter, L. Surpassing 10 000 identified and quantified proteins in a single run by optimizing current LC-MS instrumentation and data analysis strategy. *Mol. Omics* **2019**, 348.

(50) Collins, B. C.; Hunter, C. L.; Liu, Y.; Schilling, B.; Rosenberger, G.; Bader, S. L.; Chan, D. W.; Gibson, B. W.; Gingras, A. C.; Held, J. M.; Hirayama-Kurogi, M.; Hou, G.; Krisp, C.; Larsen, B.; Lin, L.; Liu, S.; Molloy, M. P.; Moritz, R. L.; Ohtsuki, S.; Schlapbach, R.; Selevsek, N.; Thomas, S. N.; Tzeng, S. C.; Zhang, H.; Aebersold, R. Multi-laboratory assessment of reproducibility, qualitative and quantitative performance of SWATH-mass spectrometry. *Nat. Commun.* **2017**, *8*, No. 291.

(51) Smeal, T.; Binetruy, B.; Mercola, D. A.; Birrer, M.; Karin, M. Oncogenic and transcriptional cooperation with Ha-Ras requires phosphorylation of c-Jun on serines 63 and 73. *Nature* **1991**, *354*, 494–496.

(52) Jaeschke, A.; Karasarides, M.; Ventura, J. J.; Ehrhardt, A.; Zhang, C.; Flavell, R. A.; Shokat, K. M.; Davis, R. J. JNK2 is a positive regulator of the cJun transcription factor. *Mol. Cell* **2006**, *23*, 899–911.

(53) Shen, R. R.; Zhou, A. Y.; Kim, E.; Lim, E.; Habelhah, H.; Hahn, W. C. I κ B kinase epsilon phosphorylates TRAF2 to promote mammary epithelial cell transformation. *Mol. Cell. Biol.* **2012**, *32*, 4756–4768.

(54) Blackwell, K.; Zhang, L.; Thomas, G. S.; Sun, S.; Nakano, H.; Habelhah, H. TRAF2 phosphorylation modulates tumor necrosis factor alpha-induced gene expression and cell resistance to apoptosis. *Mol. Cell. Biol.* **2009**, *29*, 303–314.

(55) Haas, T. L.; Emmerich, C. H.; Gerlach, B.; Schumke, A. C.; Cordier, S. M.; Rieser, E.; Feltham, R.; Vince, J.; Warnken, U.; Wenger, T.; Koschny, R.; Komander, D.; Silke, J.; Walczak, H. Recruitment of the linear ubiquitin chain assembly complex stabilizes the TNF-R1 signaling complex and is required for TNF-mediated gene induction. *Mol. Cell* **2009**, *36*, 831–844.

(56) Pescatore, A.; Esposito, E.; Draber, P.; Walczak, H.; Ursini, M. V. NEMO regulates a cell death switch in TNF signaling by inhibiting recruitment of RIPK3 to the cell death-inducing complex II. *Cell Death Dis.* **2016**, *7*, No. e2346.

(57) Nakazawa, S.; Oikawa, D.; Ishii, R.; Ayaki, T.; Takahashi, H.; Takeda, H.; Ishitani, R.; Kamei, K.; Takeyoshi, I.; Kawakami, H.; Iwai, K.; Hatada, I.; Sawasaki, T.; Ito, H.; Nureki, O.; Tokunaga, F. Linear ubiquitination is involved in the pathogenesis of optineurin-associated amyotrophic lateral sclerosis. *Nat. Commun.* **2016**, *7*, No. 12547.

(58) Annibaldi, A.; Wicky John, S.; Vanden Berghe, T.; Swatek, K. N.; Ruan, J.; Liccardi, G.; Bianchi, K.; Elliott, P. R.; Choi, S. M.; Van Coillie, S.; Bertin, J.; Wu, H.; Komander, D.; Vandenabeele, P.; Silke, J.; Meier, P. Ubiquitin-Mediated Regulation of RIPK1 Kinase Activity Independent of IKK and MK2. *Mol. Cell* **2018**, *69*, 566.e5–580.e5.

(59) Wagner, S. A.; Satpathy, S.; Beli, P.; Choudhary, C. SPATA2 links CYLD to the TNF-alpha receptor signaling complex and modulates the receptor signaling outcomes. *EMBO J.* **2016**, *35*, 1868–1884.

(60) Chan, F. K.; Luz, N. F.; Moriwaki, K. Programmed necrosis in the cross talk of cell death and inflammation. *Annu. Rev. Immunol.* **2015**, *33*, 79–106.